Structural Eng./Earthquake Eng., JSCE, Vol. 14, No. 1, 83s—93s, 1997 April

# FIELD VIBRATION TEST OF A LONG-SPAN CABLE-STAYED BRIDGE USING LARGE EXCITERS

Isao OKAUCHI[1], Toshio MIYATA[2], Masaaki TATSUMI[3] and Nobuyuki SASAKI[4]

[1]Fellow member of JSCE, D. Eng., Professor, Dept. of Civil Eng. Cyuo University (13-27, Kasuga 1, Bunkyo-ku, Tokyo 112, Japan)
[2]Member of JSCE, D. Eng., Professor, Dept. of Civil. Eng.. Yokohama National University (156, Tokiwadai, Hodogaya-ku, Yokohama 240, Japan)
[3]Member of JSCE, D. Eng., Honshu-Shikoku Bridge Authority (1-5, Toranomon 5, Minato-ku, Tokyo 105, Japan)
[4]Member of JSCE, Hiroshima R.&.D Center, Mitsubishi Heavy Industries, Ltd. (5-1, Ebaoki, Naka-ku, Hiroshima 730, Japan)

This paper presents the results of a field vibration test and numerical analysis of a long-span cable-stayed bridge. In the test, large exciters were used to vibrate the bridge to a certain level of amplitude. Dynamic properties, especially damping at large amplitudes, in the lower significant modes of the bridge were measured. By the comparison of the measured values with assumed ones at the design of these properties, dynamic design of the bridge was verified. In addition, coupled vibration between the girder and the cables which was observed in the field test was investigated by conducting a numerical analysis of the bridge.

*Key Words*: *cable-stayed bridge, field vibration test, dynamic properties, coupled vibration*

## 1. INTRODUCTION

One of the most important tasks in the design of long-span cable-stayed bridges is to ensure an adequate level of safety against dynamic loadings such as strong wind and earthquakes. This can only be achieved if the dynamic properties of the bridge such as natural frequency, mode shapes and structural damping are accurately modeled during design.

However, an analytical evaluation of structural damping is very difficult. Therefore, the validity of the assumed structural damping used in the design can only be verified through field vibration tests after the completion of the bridge.

It is also known that the structural damping in general varies with the amplitude of vibration, but the amplitude dependence of damping is not fully understood[1]. Therefore, one of the goals of our field vibration tests was to investigate damping properties at large amplitude.

Another difficult aspect of the dynamic behavior of cable-stayed bridges is coupled vibration between the girder and cables[2]. As there are relatively few examples of field investigations of this behavior, its properties remain unclear. This coupled behavior can be studied effectively only if the bridge is vibrated with large amplitudes.

The above issues were kept in mind when we set out to conduct a field vibration test on the Hitsuishijima Bridge, one of the Honshu-Shikoku Bridges, using large exciters just before the bridge went into service.

In this paper we discuss the following topics:

1. Comparison of structural damping used in the design of the bridge with the measured values obtained from field tests using large amplitude excitations (maximum amplitude of stiffening girder was about 10 cm).

This paper is translated into English from the Japanese paper, which originally appeared on J. Struct. Mech. Earthquake Eng., JSCE, No. 507/I-30, pp. 65 - 75, 1995. 1.

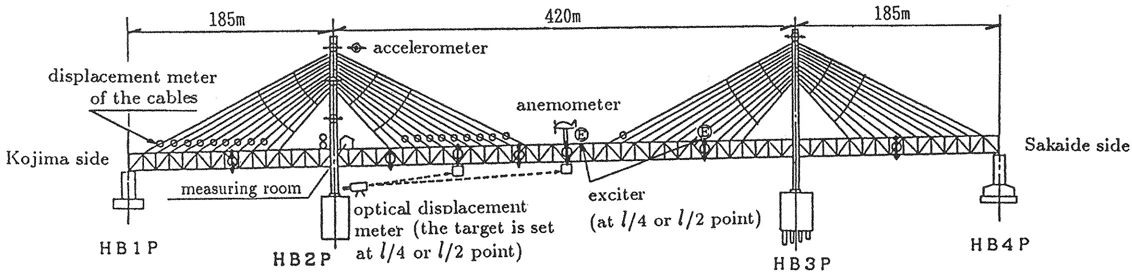


**Fig.1** Subject bridge and measuring points

**Table 1** Specification of the exciter

| | |
|---|---|
| exciting direction | vertical |
| total weight | about 110tf + foundation 14tf |
| size | H=6.30m, W=6.10m, L=7.10m |
| sliding mass | 55.50 to 6.00 tf |
| mass stroke | ±0.16m |
| frequency range | 0.36 to 2.17 Hz |
| generated wave | approximated sinusoidal wave |
| exciting force | maximum 20tf (0.7 Hz or over) |
| brake device | quick stop by disc brakes |

2. Verification of the model used in the design by a comparison of the design and measured values of the natural frequencies and mode shapes of the lower significant modes.
3. Investigation of the dynamic interaction between the girders, cables and towers.

## 2. THE HITSUISHIJIMA BRIDGE

The Hitsuishijima Bridge is a 3-span continuous steel bridge with an overall length of 790m (185 m + 420 m + 185 m) and its main tower height rises 152m above sea level. This bridge is one part of the Kojima-Sakaide route of the Honshu-Shikoku Bridge, connecting the Hitsuishi and the Iwaguro islands. A general view of the bridge is shown in **Fig.1.** The structural outline of the bridge is as follows:

1. The stiffening girder is a Warren truss with vertical members. The girder carries two decks: an upper deck is a highway and the lower deck has a rail line which are in use and a spare line for future use for the Shinkansen Line.
2. The tower is a two-story rigid frame supported on columns with haunches for aesthetic reasons. The columns have a varying cross-section with two-way taper.
3. The cable is a eleven-step multi-fan type in both planes. As a preventive measure against wind-induced vibration, the cables of each step are tied to one another by wire ropes at two points as shown in **Fig.1.**

## 3. TESTING PROCEDURE

### (1) Exciting Procedure

The exciters are a pair of large-scale exciters specially made for the field vibration test of the Honshu-Shikoku Bridge.

The exciters were originally designed for lower frequency excitation of suspension bridges[3)], and required partial remodeling for testing the Hitsuishijima Bridge. **Table 1** shows the specification of the remodeled exciters.

The exciters are driven by a crank mechanism which transforms the rotational motion of a D.C. motor into vertical motion of the mass. As a result of the crank mechanism, the exciting force has two frequency components: a primary component at the driving frequency $f$ and a secondary component at twice the frequency, $2f$. The exciters used in the test had about 10% of the total exciting force in the secondary component at frequency $2f$.

Two similar exciters were placed at both ends of the cross-section of the bridge and they were operated in-phase or out-of-phase to excite vertical bending vibration and torsional vibration, respectively. As regards their position in the longitudinal direction, they were first installed at quarter-point of the midspan and then shifted to mid-point to excite asymmetric mode and symmetric mode, respectively.

### (2) Measuring Procedure

The locations of transducers are shown in **Fig.1.** Vertical vibration of the girders and flexural vibration of the towers in the direction

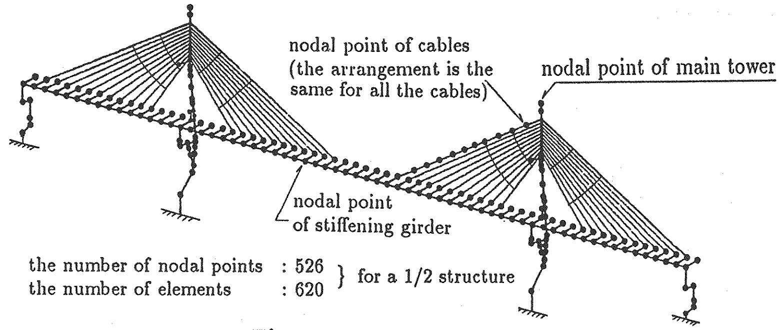


**Fig.2** Analytical model

of the bridge axis were measured by a servo-type accelerometer (24 components in total). As for the cables, 19 were selected for measurement of vertical (in-plane) displacement using variable-resistance displacement meters.

Also, in order to observe the behavior of sliding parts, the rotational displacement at the tower links and lateral sliding displacement at the girder ends were measured by strain-gauge-type displacement meters. The displacement of the girder was measured by an optical displacement meter.

In addition to the above measurements, we also set a servo-type accelerometer to the exciter's mass so that in the tests we could obtain an accurate phase relation between the exciting force and the response.

For reference, wind velocity and direction on the bridge surface and the temperature of the bridge body were measured.

### (3) Data Analysis Procedure

We used a data processing system consisting of a high-speed, high-performance 32-bit engineering workstation in a measuring room on the bridge. The workstation was used for on-line data collection and data reduction of raw data gathered from all transducers, to monitor the modal circles of frequency response, and carry out other major data processing. As data was being continuously monitored, we were able to keep to a minimum the number of large amplitude loading repetitions so as to avoid causing any damage to the bridge during the test.

As for the frequency response data, the data was digitally filtered to exclude all frequency components other than the primary excitation frequency $f$, regarding the response of other frequency components as noise. This enabled us to eliminate the effect of the secondary excitation $2f$.

## 4. NUMERICAL ANALYSIS

A three-dimensional model of a coupled system consisting of girders, towers and cables was used to perform a natural vibration analysis. The various components of the model for representing the Hitsuishijima Bridge are:

1. girder modeled by beam elements with rigidities equivalent to those of the trussed structure,
2. main tower and pier by beam elements, and
3. cable by cable elements. (Nodal points distributed the cables as shown in **Fig.2**. The mass is distributed, and the nodal points are linked to one another with axial rigidities and lateral rigidities which are defined by the initial tension.)

We have used conventional techniques[4] for modeling girder, tower and pier and it is in modeling the cable that we have used a more detailed model to make it possible to examine the interaction between the cable and other members. The number of nodal points which are required to analyze the vibration of the cable up to a maximum frequency of 2 Hz detected in our field test was determined by a preliminary analysis. The model shown in **Fig.2** is symmetric about the center line, therefore we used half the structure and adopted either symmetrical or asymmetrical boundary conditions for investigating vertical bending and torsional vibrations, respectively.

## 5. TEST RESULTS AND DISCUSSIONS

### (1) Natural frequency and vibration mode

**Fig.3** shows typical examples of frequency response analyses. **Figs.3(a)** and **3(b)** show amplitude response curves and phase response curves, respectively. The phase response curves of **Fig.3(b)** show the phase lag of the bridge re-

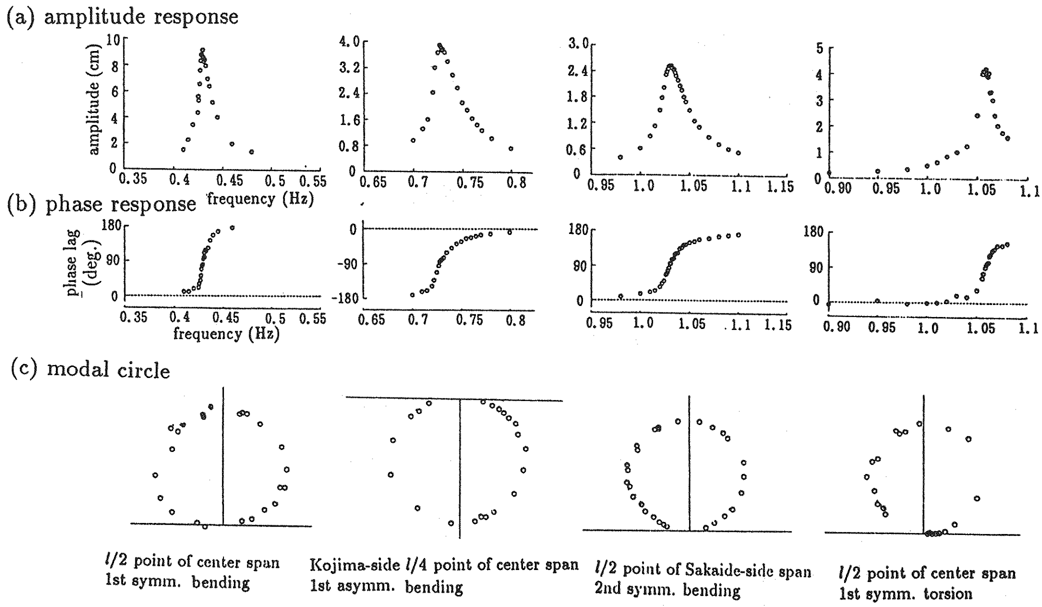


**Fig.3** Frequency response

sponse with respect to the exciting force. The exciting force was calculated by multiplying the weight of the mass by the relative acceleration which was obtained by subtracting the acceleration of the girder at the same location as the exciter from the absolute acceleration of the exciter weight. **Fig.3(c)** shows polar plots[5] of amplitude and phase. In our frequency response analysis we have paid attention not only on amplitude response but also on phase data by examining phase response and polar plots of amplitude and phase in order to obtain more accurate results at around resonance points.

In dynamic tests of bridges or other structures with small damping, the maximum amplitude at resonance points may not always be detected clearly because the frequency pitch of the exciter is not small enough. In such a case, amplitude data may not provide clear information about resonance frequency and maximum amplitude at resonance, with the possible result that the damping gets overestimated. On the other hand, when we analyze data using polar plots of amplitude and phase the fact that at around resonance the polar plots become almost perfect circles makes it possible to estimate damping with a relatively high accuracy, even if data at exactly the resonance point is missing.

As can be seen in **Fig.3**, the relation between phase and maximum amplitude are almost perfect circles in the test. Similar results were obtained at other modes.

**Table 2** lists the measured and numerically calculated values of natural frequencies. The measured values correspond well with calculated values and the error doesn't exceed 5%, except for an error of 11% found in the 1st asymmetric torsional vibration.

**Fig.4** shows the numerically calculated and measured mode shapes of girder and tower at resonance. As can be seen from this figure, the two correspond with each other for all modes.

### (2) Structural Damping

The three methods used in our study for calculating structural damping are:

1. Free vibration tests after a sudden stop of the exciter at resonance.
2. Half-power method, using a least squares method of the polar plot[5] of amplitude and phase.
3. Back calculation from the maximum amplitude of frequency response at resonance.

Methods 1 and 2 are used for test data while Method 3 is used to analyze the results of natural vibration analysis.

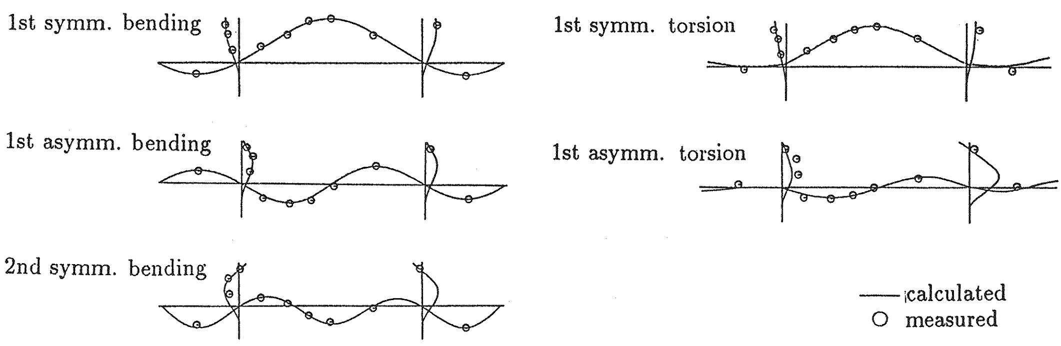


**Fig.4** Mode shapes

**Table 2** Test results

| vibration mode | | frequency calculated (Hz) | frequency measured (Hz) | logarithmic decrement $\delta$ | maximum amplitude displace-ment (cm) | maximum amplitude rotation (deg) | exciter |
|---|---|---|---|---|---|---|---|
| bending | 1st symm. | 0.429 | 0.430 | 0.080 | 9.12 | — | $\ell/2$ |
| | 1st asymm. | 0.734 | 0.729 | 0.088 | 3.88 | — | $\ell/4$ |
| | 2nd symm. | 1.080 | 1.030 | 0.066 | 2.52 | — | $\ell/2$ |
| torsion | 1st symm. | 1.029 | 1.058 | 0.046 | 4.21 | 0.175 | $\ell/4$ |
| | 1st asymm. | 1.715 | 1.910 | 0.071 | 0.37 | 0.015 | $\ell/4$ |

**Fig.5** shows a typical example of free vibration data. As a whole, the quality of wave patterns are good except in the 1st asymmetric torsional vibration, whose pattern was affected by large vibration of cables. The details of this behavior are discussed in Chapter 6(2).

**Fig.6** shows typical example of circles fitted to the polar amplitude-phase data.

**Fig. 7** shows the structural damping obtained by all three methods plotted against girder amplitude to examine its amplitude dependence. Also, the results of the free vibration tests conducted under various weather conditions are superimposed in order to check the reproducibility of the estimated damping. The structural damping estimated from the amplitude-phase curves are plotted at a 1/2 point of the maximum amplitude at resonance point.

As can be seen in **Fig. 7**, the structural damping estimated using the three methods correspond very well with each other, indicating that the estimated structural damping is highly reliable.

Also, as seen in **Fig. 7**, the amplitude dependence of damping varies with vibration mode. A noticeable dependence is found in the 1st symmetric bending vibration, for which the structural damping nearly doubled as the girder amplitude increased.

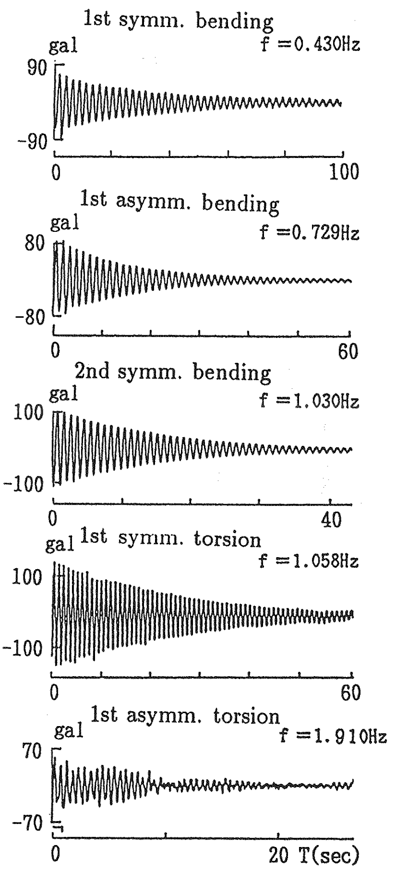


**Fig.5** Free vibration

On the other hand, structural damping in other modes was relatively constant with

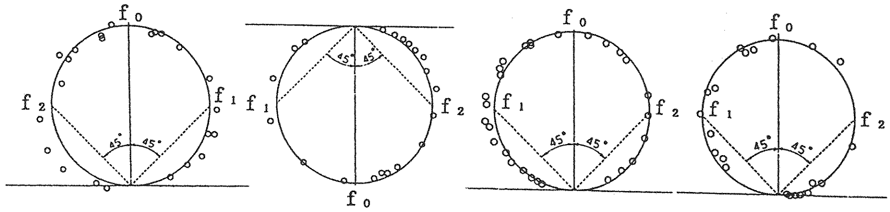


**Fig.6** Modal circle fitting

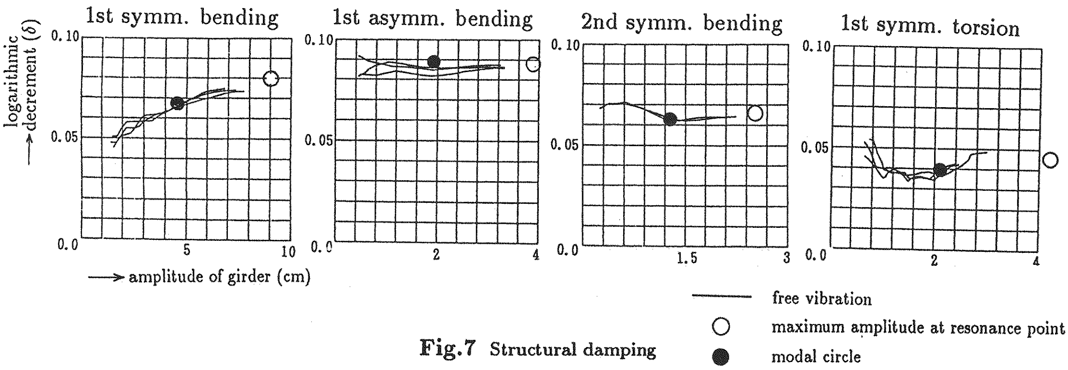


**Fig.7** Structural damping

change in girder amplitude. In our test the exciter was used all the way up to its maximum power at which the maximum amplitude of the girders was as shown in **Table 2**.

The weather conditions under which the free vibration tests of the 1st symmetric bending vibration mode shown in **Fig.7** were conducted are listed in **Table 3**. Although the limited data set collected in our tests are not sufficient to establish a definitive relation between weather conditions and damping, the reproducibility of structural damping is satisfactory. Therefore, the estimated structural damping is considered to be reliable, not being significantly affected by wind velocity, wind direction and temperature. For more details of these test results, see our former reports[11),12)].

So far, we have examined the vibration properties of the stiffening girder, however the behavior of cables was found to be more complicated. As we had used only a limited number of transducers on the cable, we were not able to observe the details of the complicated vibration of cables in this test. However, some interesting interaction between the girder and the cables was found at around the natural frequency of the girder. This point is examined in the following sections.

## 6. COUPLED VIBRATION OF GIRDER AND CABLE

### (1) Mode separation of the coupled free vibration

When the natural frequencies of the girder and the cable are close to each other, their free vibrations may interfere to form a beat-shaped vibration, a phenomenon known as dynamically coupled vibration.

In our test, we observed coupled vibration under certain conditions. For instance, when the cables were excited at around the 1st symmetrical torsional mode by the exciter installed at mid-point, the top cable vibrated greatly. The free vibrations of the girder and the cable interfered with each other, forming a coupled vibration form as shown in **Fig.8**. On the other hand with the exciter at quarter-point, no interaction between the cable and girder was observed with only a regular type of free vibration as shown in **Fig.5**. This difference in behavior can be explained as a result of the

**Table 3** Weather conditions at the time of the test (1st symm. bending)

| TestNo. | wind velocity (m/s) | wind direction $\theta$ | temperature of bridge($^{\circ}C$) |
|---|---|---|---|
| 1st test | 9.1 | 40 | 9.6 |
| 2nd test | 6.5 | 62 | 10.6 |
| 3rd test | 5.1 | 1.86 | 6.5 |

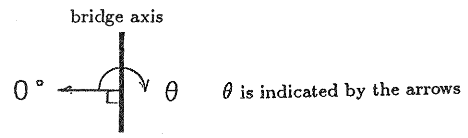


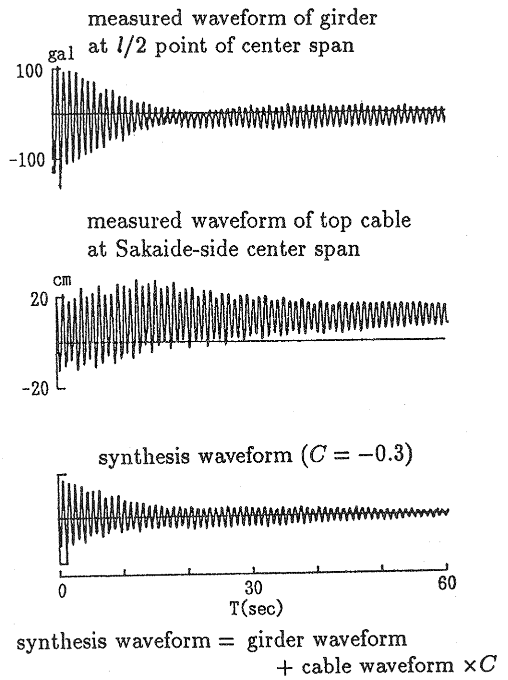


**Fig.8** Girder-cable coupled waveform and separated waveform

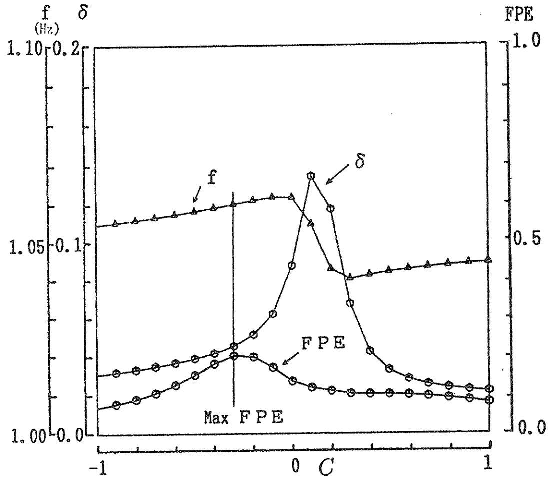


**Fig.9** Mode separation by MEM

change in cable tension because of the shift in the location of the exciter. The change in cable tension caused a change in the natural frequency of the cable and therefore the ratio of natural frequency of girder to cable was modified.

As the interaction between the girder and cable was minimal when the exciter was placed at quarter-point, we adopted its data to estimate the dynamic properties in the 1st symmetric torsional vibration.

For the sake of reference, we went ahead and analyzed the data of the 1st symmetric torsional vibration obtained with the exciter installed at mid-point in which case the interaction between the girder and the cable was observed. There are several established methods[6),7)] for estimating structural damping from a beat-shaped free vibration record.

These methods calculate damping from the beat cycle and the maximum value of the beat envelope, and are therefore not suitable to waveforms with unclear beat cycle. Therefore, we digitized the measured free vibration waveforms of the cable and girder, then separated the modes from each other to obtain the damping of the girder. The digitized record was first high pass filtered to eliminate low frequency noise and the acceleration time history of the girder was integrated twice to get a displacement time history.

To separate the modes, the vibration record of the cable was multiplied by a constant $C$ and added to the vibration record of the girder to derive a synthetic waveform. The summation of the two waveforms was repeatedly performed using various $C$'s. With $C$ at a value of $C_1$, the synthetic waveform became closer to the free vibration waveform of the girder and at $C_2$ closer to the free vibration of the cable. Although $C$ is an arbitrary constant, when only the cable vibration mode is obtained and the maximum value of free vibration waveforms of cable and girders is normalized to 1.0, the range of $C$ is limited to lie between 0 and $\pm$ 1.0.

In order to determine the optimum $C$, a multiple regression analysis was performed on the assumption that the measured waveform consists of two vibration components and white noise. Prior to the regression analysis,

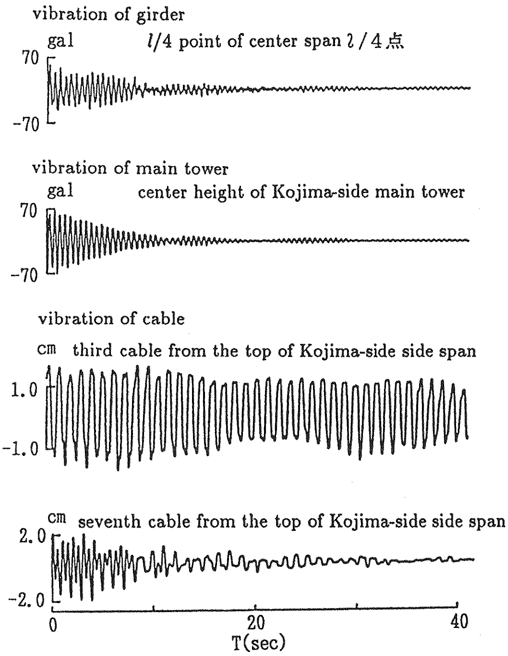


**Fig.10** Free vibration in 1st asymm. bending mode

vibration waveforms of the girder and the cable were summed with a certain value of $C$ to generate a synthetic waveform $y$. Then, in order to fit this waveform to a form of a single mode free vibration as expressed in Eq. (1), multiple regression analysis was conducted to determine $y'$.

$$y' = e^{-h\omega t}(A\cos\omega_d t + B\sin\omega_d t) \qquad (1)$$

here, $\omega_d = \sqrt{(1-h^2)} \times \omega$

$\omega$ : natural frequency
$h$ : damping constant $=\delta/2\pi$
A,B : unknown variables

Next, the spectrum of the error waveform $(y - y')$ was analyzed by Maximum Entropy Method (MEM)[8] and the error tested by Akaike's Final Prediction Error[8]. The analyses was repeated with various values of $C$ until an optimum $C$ was found at which the level of white noise became maximum. The analytical result is graphed in **Fig.9**. It is seen from this figure that when the maximum FPE was obtained at $C_1$=-0.3, the frequency of the synthesized waveform was 1.06 Hz, and its damping

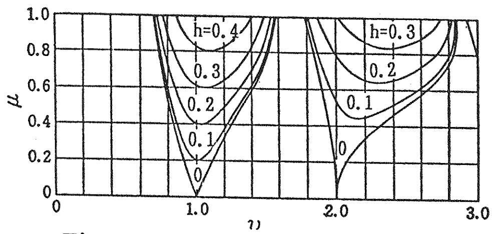


**Fig.11** Dynamic instability curves of cables

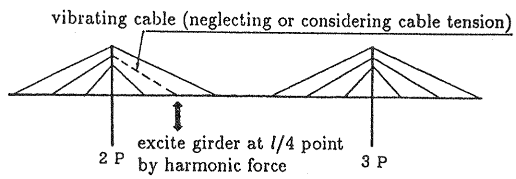


**Fig.12** Analytical model

about $\delta$=0.045. These values correspond well with those of the first symmetrical torsional vibration obtained with the exciter installed at quarter-point, thereby proving the validity of this method.

## (2) Influence of the Fluctuation in Cable Tension

As mentioned in section 5.(2), the free vibration of the stiffening girder in the first asymmetrical torsional vibration was considered to be affected by the vibrations of the cables. Here, an unique phenomenon was observed in the vibration of the cable, which is assumed to be the effect of fluctuation in cable tension.

**Fig.10** shows typical examples of free vibration of the girder, main tower and cable. The frequency of excitation (1.9 Hz) is dominant in the vibration of the girder and tower, whereas the cable vibrates largely with half the frequency of excitation. This phenomenon can be explained as resulting from dynamic instability of the cable.

When a cable tension is fluctuated, the vibration of string of the cable can be expressed by the following Hill-type equation (2):

$$\frac{\partial^2 y}{\partial t^2} - \lambda^2(1 - \frac{\Delta T}{T_0}\cos\omega t)\frac{\partial^2 y}{\partial x^2} = 0 \qquad (2)$$

where, $\lambda^2 = \frac{T_0}{\rho}$

$T_0$ : static tension (pre-tension)
$\rho$ : mass of unit length
$\Delta T\cos\omega t$ : fluctuation in tension

The variable $y(x,t)$ can be separated and transformed into modal variables $\phi_j(t)$ of each cable. Then, by defining a damping constant

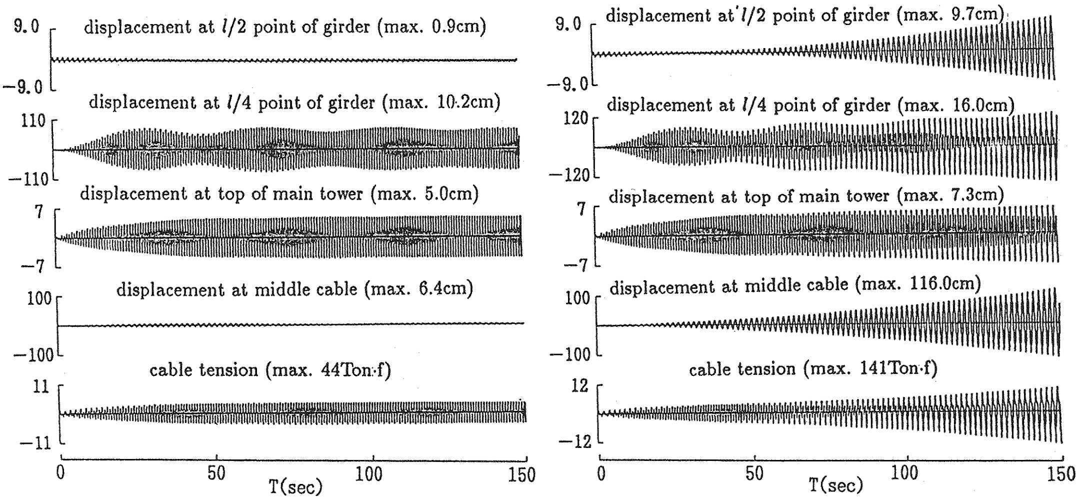


(a) ordinaly analysis (neglecting cable tension)

(b) parametric excitation analysis (considering cable tension)

**Fig.13** Time history response to harmonic excitation

$h_i$ of cable damping as modal damping, Eq.(2) can be re-written as Eq.(3), as follows:

$$\phi_i + 2h_i v_i \phi_i + v_i^2(1 - 2\mu\cos 2\tau)\phi_i = 0 \quad (3)$$

where, $v_1 = \frac{\omega_i}{\omega}$
$\omega_i$ : $i$th frequency of vibration of string
$\frac{\Delta T}{T_0} = 2\mu$
$\tau = \omega t$

Solving Eq.(3), both stable and unstable solutions can be obtained and are shown by the dynamic instability curves of **Fig.11**[9]. It is clear from **Fig.11** that when the natural frequency of vibration of string is close to half the frequency of the tension, the unstable region of the cable widens; moreover, the divergence from a stable solution is more likely to occur for larger fluctuations of tension and smaller structural damping.

If the cable vibration becomes unstable, then the entire structural system of cable-stayed bridges can become dynamically unstable. This phenomenon has never been reported in the previous experiments[13)−16)]. Our experiment is the first confirmation of this phenomenon in an actual bridge. This behavior is considered to be one of the causes for the insufficient correspondence between the measured and numerically calculated natural frequencies of the asymmetrical torsional mode.

In order to further investigate the effects of unstable vibration of cable on the vibration response of the bridge, we carried out response analyses using a simplified model of a cable-stayed bridge.

**Fig.12** shows a 2-D model of a cable-stayed bridge of the size of Hitsuishijima Bridge. It has 12 cables modeled by three cable elements. The tension fluctuation was modeled in only the middle cable and the rest were treated as simple axial members. The ratio of natural frequencies of the girder and cable was adjusted as follows:

(1) The natural frequency of the first asymmetrical bending vibration of the girder was taken to be twice as large as that of the first symmetrical vibration.
(2) The first mode frequency of the middle cable was made to correspond with the first symmetrical frequency of the girder and the second mode frequency correspond with the first asymmetrical frequency of the girder.

The above-mentioned frequency ratios were selected so that the vibration of the cable is likely to be unstable and its vibration likely to affect the girder vibration. The structural damping of the girder and cable were set at 0.05 and 0.005 in logarithmic decrement, respectively. As for exciting force, a concentrated harmonic force was applied to the model at quarter-point of the girder. The frequency of the harmonic force was set at 1.18 Hz, which almost corresponds with the first asymmetrical frequency of the girder (or the second asymmetrical frequency of the cable.) In order to emphasize the dynamic instability, the amplitude of the exciting force was set at five times larger than the experimental one.

Two kinds of response analyses were carried out: a simplified analysis neglecting cable tension, and the other a parametric excitation analysis considering cable tension. By comparing the output of these two models, the effect of fluctuation in cable tension in the overall dynamic behavior was examined.

The parametric excitation analysis considering the fluctuation in cable tension was done by a time-stepping analysis using Newmark's $\beta$ method ($\beta$=1/6) to solve the equation of motion of the bridge. However, as the computations would be numerically very intensive a super-block method[10] was applied, in which the whole structure was divided into cable elements and other elements. The unknown variables of cable elements were transformed into modal variables using modal analysis; while, variables of the other elements were reduced using mass condensation[10].

The results of the time history analyses with and without considering cable tension are shown in **Figs.13** (a) and (b), respectively. In the analysis neglecting cable tension, the response at every point has the same frequency component as the exciting frequency. The girder vibrates at the first asymmetrical mode and the cable vibrates at the second mode. The amplitude of the vibration reaches the stationary state after 150 seconds of applying the load.

On the other hand, in the analysis considering cable tension, a considerable increase in the frequency component equal to half the exciting frequency can be recognized in the response of the girder and cable specially as the amplitude increases. The amplitude in this case is relatively larger than the one in the analysis neglecting the cable tension. Even after 150 seconds, the amplitude continues to increase and the vibration of girder appears to be sliding to the unstable region.

Judging from the results of the field tests and numerical analyses, it can be concluded that the unstable behavior of the cable of a cable-stayed bridge may lead to a large vibration of the entire bridge.

As cable-stayed bridges become longer and bigger, the problem concerning the stability of cable becomes even more serious. In cases of dynamic loading such as strong wind or earthquakes, it is necessary to examine the instability of cables arising from fluctuations in cable tension. In these situations preventive measures such as increasing structural damping of the cable may need to be required.

The numerical model used in the analysis was by necessity a simplified model and it does not account for cable sag and nonlinearities arising from large deflections[2]. Therefore, the complexities observed in the tests couldn't be fully simulated by the numerical model. This paper has attempted to explain one aspect of dynamic interaction observed in the experiments, and has highlighted the possibility that this phenomenon can lead to a vibration problem of long-span cable-stayed bridges. The effects of the non-linear terms not included in this study will be the subject for future investigations.

## 7. CONCLUSION

From the experimental results, we can conclude the following:

(1) The measured values of structural damping $\delta$ in logarithmic decrement, which is the most significant data collected in this experiment, varied from $\delta$= 0.06 to 0.09 for bending vibration and from 0.04 to 0.07 for the torsional vibration. These values are larger than the design value of $\delta$=0.03 specified in a wind resistant design code for Honshu-Shikoku Bridge. The estimated damping values were insensitive to weather conditions (temperature, wind velocity, etc.) during the test.

(2) When the amplitude is smaller than the maximum amplitude of 10cm in the experiment, the amplitude dependence of damping varies with the vibration mode. A noticeable amplitude dependence is found only in the first symmetrical bending mode for which the structural damping increases from 0.05 to 0.08 with increase in girder amplitude.

(3) The structural damping estimated using the circle fitted to the polar plot of amplitude and phase was in good agreement with the damping estimated from free vibration data.

(4) The estimated values of natural frequencies and mode shapes of the significant, lower modes matched well with the respective values calculated from the numerical model. The highest difference between the test and numerical results was found in the first asymmetrical torsional vibration for which the difference in the natural frequencies was about 10%. This is most likely the effect of unstable vibration of the cable.

(5) When the natural frequencies of the girder and cable are close to each other, their free vibrations interfere with each other to form a beat-shaped waveform. A synthetic waveform calculated by multiple regression analysis was seen to be effective in separating the free vibration of the girder from the record of coupled vibration. This method is considered to be effective for separating the coupled vibration even when the beat frequency is unclear The damping estimated from the separated time histories was seen to be comparable to values estimated from other methods.

(6) At the point of resonance of the first asymmetrical torsional vibration, the cable vibrated with large amplitudes at half the exciting frequency. This vibration of the cable is considered to be parametric oscillation caused by fluctuation in cable tension. A frequency response analysis considering parametric excitation resulting from fluctuation in cable tension was carried out using a simplified model of a cable-stayed bridge. The results of the analysis suggest that the unstable vibration of the cable has the possibility of leading to an increase in the response of the bridge. Therefore, in the future, it is desirable to consider the stability of cables in the design of long-span cable-stayed bridges.

**ACKNOWLEDGMENTS:** The authors would like to thank the members of the Honshu-Shikoku Bridge Wind Resistance Committee for their guidance and the staff in the Joint Ventures of Construction for their cooperation in carrying out the experiment.

## REFERENCE


1) M. Ito, et al.: Damping of Bridge Structures, *Proc. of JSCE*, No.117, pp.12-22, May, 1965 (in Japanese).
2) P. Warnitchai, et al.: Analysis and Experiment on Dynamics of a Cable-Girder System with Emphasis on Linear and Nonlinear Coupling, *Journal of Structural Eng*, Vol.36A, pp.719-732, Mar. 1990 (in Japanese).
3) I. Okauchi, et al.: Dynamic Field Tests and Studies on Vibrational Characteristics of Long-Span Suspension Bridges, *Proc. of JSCE*, No. 446/I-19, pp. 89 - 100, Apr. 1992.
4) I. Konishi: *Steel Bridges, Design Part I*, Maruzen, pp.597-628, 1975 (in Japanese).
5) I. Nagamatsu: *Modal Analysis*, Baifukan, pp.107-112, 1985 (in Japanese).
6) H. Shibata, et al.: Analysis of Decrement Waveform with Beating, it Seisankenkyu, Vol.17, No.8, pp.13, Aug. 1969 (in Japanese).
7) Y. Sanuki, et al.: Calculation Methods of Logarithmic Decrement from Beating Waveform, *Proc. of 2nd. Colloquium on Bridge Traffic Vibration*, pp. 109 - 114, Aug. 1989 (in Japanese).
8) M. Hino: *Spectral Analysis*, Asakurasyobo, pp.86-88, pp.210-225, 1989 (in Japanese).
9) O. Taniguchi: *Handbook of Vibrational Engineering*, Yokendo, pp.447-452, 1988 (in Japanese).
10) K. Washizu. et al.: *Handbook of Finite Element Method II, Application Part*, Baifukan, pp.5-7, 1983 (in Japanese).
11) N. Sasaki, et al.: Field Vibration Test of the Hitsuishijima Bridge, *Proc. of 43rd Annual Conf.* of JSCE. I, pp.634-634, Oct. 1988 (in Japanese).
12) T. Ota, et al.: Vibration Test on Aerodynamic Stability of Hitsuishijima Bride (Cable-Stayed Bridge), *Honshu-Shikoku Bridge Authority Reports*, Vol. 13, No.48, pp.12-21, Oct. 1988 (in Japanese).
13) H. Yoshikawa, et al.: Field Vibration Test of S-Shape Curved Cable-Stayed Bridge, *Proc of 42nd Annual Conf. of JSCE.* I, pp.742 743, Sept. 1987 (in Japanese).
14) K. Uno, et al.: Dynamic Properties and Suppressive Effect of Stay Cable with Dampers of Aratsu Bridge, *Proc. of 44th Annual Conf. of JSCE.* I, pp.28-29, Oct. 1989 (in Japanese).
15) H. Hayashi, et al.: Vibration Test of the Yokohama Bay Bridge, *Proc. of 45th Annual Conf. of JSCE.* I, pp.28-29, Sept. 1995 (in Japanese).
16) M. Kamei, et al.: Field Vibration Test of Sugawarashirokita Bridge, *Proc. of 45th Annual Conf. of JSCE.* I. pp.772-773, Sept. 1995 (in Japanese).